The EMBO Journal (2004) 23, 2972–2981 | © 2004 European Molecular Biology Organization | All Rights Reserved 0261-4189/04
www.embojournal.org

THE EMBO JOURNAL

The carboxy-terminal portion of TnsC activates the Tn7 transposase through a specific interaction with TnsA

Donald R Ronning[1], Ying Li[2], Zhanita N Perez[1], Philip D Ross[1], Alison Burgess Hickman[1], Nancy L Craig[2] and Fred Dyda[1,*]

[1]Laboratory of Molecular Biology, National Institute of Diabetes and Digestive and Kidney Diseases, Bethesda, MD, USA and [2]Department of Molecular Biology and Genetics, Johns Hopkins School of Medicine, Howard Hughes Medical Institute, Baltimore, MD, USA

Tn7 transposition requires the assembly of a nucleoprotein complex containing four self-encoded proteins, transposon ends, and target DNA. Within this complex, TnsC, the molecular switch that regulates transposition, and TnsA, one part of the transposase, interact directly. Here, we demonstrate that residues 504–555 of TnsC are responsible for TnsA/TnsC interaction. The crystal structure of the TnsA/TnsC(504–555) complex, resolved to 1.85 Å, illustrates the burial of a large hydrophobic patch on the surface of TnsA. One consequence of sequestering this patch is a marked increase in the thermal stability of TnsA as shown by differential scanning calorimetry. A model based on the complex structure suggested that TnsA and a slightly longer version of the cocrystallized TnsC fragment (residues 495–555) might cooperate to bind DNA, a prediction confirmed using gel mobility shift assays. Donor DNA binding by the TnsA/TnsC(495–555) complex is correlated with the activation of the TnsAB transposase, as measured by double-stranded DNA cleavage assays, demonstrating the importance of the TnsA/TnsC interaction in affecting Tn7 transposition.

The EMBO Journal (2004) **23,** 2972–2981. doi:10.1038/sj.emboj.7600311; Published online 15 July 2004
Subject Categories: structural biology; genome stability & dynamics
Keywords: differential scanning calorimetry; protein–protein complex; Tn7 transposition; X-ray crystallography

Introduction

The Tn7 transposon is a mobile genetic element that encodes several proteins necessary for its excision from a plasmid carrier and subsequent integration into the *Escherichia coli* chromosome (reviewed in Craig, 2002). Four of the Tn7-encoded proteins (TnsA, TnsB, TnsC, and TnsD) work together in a highly regulated manner to achieve transposon insertion into *attTn7*, a site 20 base pairs (bp) downstream of the essential glutamine synthetase gene.

Genetic and biochemical studies have established some of the roles played by the various Tns proteins during transposition. TnsA and TnsB are the two components of the transposase that carry out the necessary DNA cutting and joining reactions at each end of the transposon. TnsA catalyzes cleavage at the 5′ ends and TnsB recognizes and cleaves specific sequences at the transposon 3′ ends (May and Craig, 1996; Sarnovsky *et al*, 1996). TnsB also carries out the subsequent strand transfer step in which each newly created 3′ OH end attacks a phosphate on the target DNA, thereby integrating the transposon.

TnsC, an ATPase, is the central regulatory molecule in Tn7 and has three roles in the control of transposition. First, TnsC is the activator of the composite TnsAB transposase (Bainton *et al*, 1993; Stellwagen and Craig, 1997b; Lu and Craig, 2000). Second, TnsC binds structurally distorted target DNA in an ATP-dependent manner (Gamas and Craig, 1992; Bainton *et al*, 1993; Rao *et al*, 2000; Kuduvalli *et al*, 2001). Third, TnsC is the key component responsible for transposition immunity (Hauer and Shapiro, 1984; reviewed in Peters and Craig, 2001), a property of Tn7 by which it avoids insertion into a target DNA molecule that already contains a copy of Tn7, an effect that extends well over 190 kb (DeBoy and Craig, 1996).

Central to the highly specific and highly regulated integration of Tn7 at the *attTn7* site is the assembly of a nucleoprotein complex, also known as the transpososome (Bainton *et al*, 1993; Skelding *et al*, 2002). *In vitro* studies have shown that only after the proper association of four Tns proteins and both target and donor DNA molecules are the steps of donor cleavage at the 5′ and 3′ ends of both DNA strands and subsequent strand transfer carried out. One of the key questions concerning the regulation of Tn7 transposition is the exact nature of protein–protein and protein–DNA interactions within the assembled nucleoprotein complex and how these interactions control the transposition reaction.

To date, only the TnsA component of the Tn7 transpososome has been structurally characterized. The crystal structure of TnsA (Hickman *et al*, 2000) revealed that its N-terminal catalytic domain is a member of the type II restriction enzyme superfamily. In contrast, sequence similarity and identification of the active site residues (Sarnovsky *et al*, 1996) indicate that TnsB is a member of the polynucleotidyl transferase superfamily defined by the core domain of HIV-1 integrase (Dyda *et al*, 1994). Structural information concerning TnsC has been more elusive, although it does possess canonical Walker A and B motifs, consistent with its ATPase activity.

The interaction between TnsC and the TnsAB transposase results in the proper orientation of donor and target DNA and activation of the 5′ and 3′ DNA cleavage activities of TnsA and TnsB, respectively. Direct binding has been observed between TnsA and TnsC, as affinity chromatography

*Corresponding author. Laboratory of Molecular Biology, NIDDK, NIH, Bldg. 5, Room 303, 5 Center Drive, MSC 0560 Bethesda, MD 20892, USA. Tel.: +1 301 402 4496; Fax: +1 301 496 0201;
E-mail: dyda@helix.nih.gov

Received: 16 March 2004; accepted: 15 June 2004; published online: 15 July 2004

demonstrates that both full-length TnsC (residues 1–555) and an N-terminally deleted TnsC (residues 294–555) interact with TnsA (Stellwagen and Craig, 2001). *In vivo* two-hybrid experiments have confirmed this observation (Y Li and NL Craig, unpublished results). Furthermore, limited protease digestion of TnsA in the presence of full-length TnsC indicated that TnsC protects the N-terminal catalytic domain of TnsA (Lu and Craig, 2000).

In an attempt to understand the structural basis of the interaction between TnsA and TnsC, we have established that only the last 52 residues of TnsC bind to TnsA. We have also determined the three-dimensional structure of this region, TnsC(504–555), bound to TnsA using X-ray crystallography. The structure suggested a mechanism by which both TnsA and a slightly longer version of the cocrystallized TnsC fragment, TnsC(495–555), which includes a cluster of basic residues, contribute to donor DNA binding. Transposon excision and DNA binding assays were used to demonstrate that indeed the C-terminal portion of TnsC aids TnsA in binding donor DNA and stimulates the transposon excision activity of TnsAB. Taken together, the results suggest a number of previously unsuspected ways in which the roles of TnsA and TnsC are intertwined to regulate important steps during Tn*7* transposition.

Results and discussion

Defining the minimal region of TnsC required for interaction with TnsA

Recombinantly expressed TnsA and TnsC form a tight complex and elute together from a gel filtration column as a symmetrical peak with a migration time consistent with a 2:2 complex. As TnsC alone elutes at a position expected for a dimer (Stellwagen and Craig, 2001), this suggests that each TnsC monomer is able to bind one TnsA molecule. This observation reconciles the monomeric state of TnsA in solution (Hickman *et al*, 2000) with the presumed need for two TnsA molecules within the transpososome for 5′ cleavage at both ends of the transposon. To define precisely the region of TnsC that interacts with TnsA, the preformed TnsA/TnsC complex was digested with papain under conditions where TnsA was relatively resistant to cleavage while TnsC was cleaved at multiple sites. Subsequent size exclusion chromatography demonstrated that only a small fragment of TnsC with an apparent molecular weight of 4.5 kDa coeluted with TnsA, whereas larger TnsC fragments (40 and 55 kDa) were not associated with TnsA (Figure 1A).

The 4.5 kDa fragment was characterized using N-terminal sequencing and matrix-assisted laser-desorption/ionization-time-of-flight (MALDI-TOF) measurements. The combined results indicated that the TnsC fragment coeluting with TnsA consisted of the C-terminal 52 residues of TnsC, amino acids 504–555. To confirm that TnsC residues 504–555 form a stable complex with TnsA, a construct was generated consisting of TnsC residues 504–555 fused to the C-terminus of thioredoxin. After purification of the fusion protein and removal of the thioredoxin domain by thrombin cleavage, TnsC(504–555) was combined with TnsA and subjected to size exclusion chromatography. TnsA and TnsC(504–555) coeluted under the same buffer conditions where full-length TnsA and TnsC form a stable complex (Figure 1B). The migration position of the complex is consistent with a 1:1 stoichiometry, a result subsequently confirmed by sedimentation equilibrium (data not shown). Taken together, these results support the interpretation that each TnsC monomer binds one TnsA molecule, and that the TnsC dimerization motif(s) are not located in TnsC(504–555).

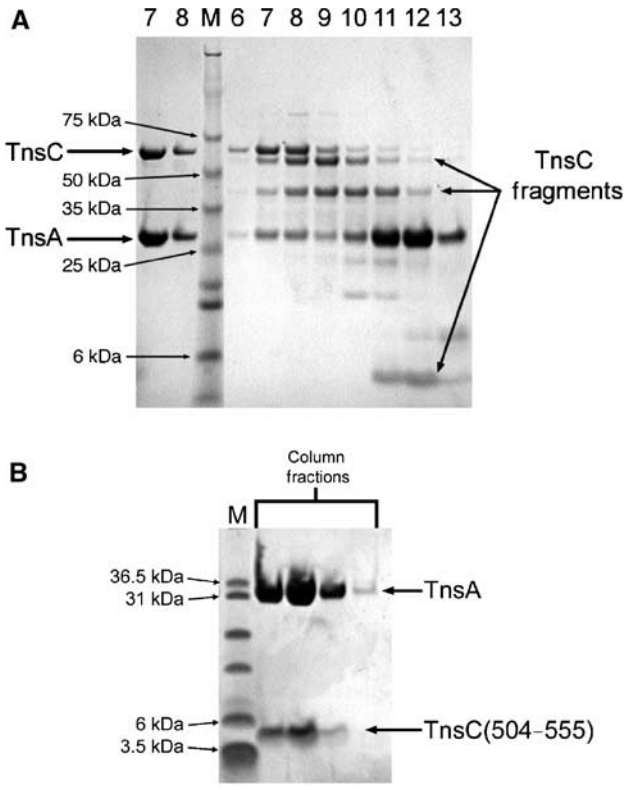

Figure 1 (**A**) Gel filtration fractions following TnsA/TnsC protease digest. Coomassie-stained gel showing fractions from a Superdex 200 (Amersham Biosciences) column following limited protease digestion. The two left-most lanes represent fractions 7 and 8 from a duplicate with undigested TnsA/TnsC. The third lane (M) is the molecular weight standard (Novagen). The remaining lanes represent fractions 6–13 where loaded protein had been previously digested with papain. (**B**) TnsA/TnsC(504–555) coelute from a gel filtration column. Coomassie-stained gradient gel. M = molecular weight marker. The lanes identified as fractions are consecutive 5 ml fractions eluting from a TSK gel filtration column.

We also performed a pull-down experiment using histidine-tagged TnsA bound to a metal affinity column and a C-terminally truncated version of TnsC, TnsC(1–503). TnsA was unable to bind TnsC(1–503) (data not shown), demonstrating that residues 504–555 of TnsC are both necessary and sufficient for the interaction between TnsA and TnsC.

Crystal structure of TnsA/TnsC(504–555)

The TnsA/TnsC(504–555) complex was crystallized and its crystal structure solved by molecular replacement using the three-dimensional structure of uncomplexed TnsA (Hickman *et al*, 2000; PDB code 1f1z) as the search model. The crystals diffracted to 1.85 Å resolution (Table I), resulting in very clear difference electron density, allowing the unambiguous interpretation and construction of the model for the TnsA/TnsC(504–555) complex (Figure 2A). The final model for TnsA includes residues 5–268, and for TnsC(504–555),

Table I Diffraction and refinement data

Data collection	
Resolution	50–1.85
Total reflections	250 124
Unique reflections	66 363
Redundancy	3.7
Completeness (%)	97.9
I/σ	9.3
R_{sym} (%)	7.8
Highest shell (1.91–1.85 Å)	
Completeness (%)	99.6
I/σ	2.37
R_{sym} (%)	38.6
Refinement	
Resolution (Å)	50–1.85
Atoms (*N*)	5463
Reflections (*N*)	66 363
R factor (%)	21.10
R_{free} (%)	23.63
R.m.s. bond length (Å)	0.005
R.m.s. bond angles (deg)	1.17
Average *B* factor (Å^2)	34.0
Average r.m.s. *B* factor bonded atoms (Å^2)	1.87

$R_{sym} = \sum|I - \langle I\rangle|/\sum\langle I\rangle$.
R factor $= \sum|FP_o - FP_c|/|FP_o|$.
R_{free} is computed using 5% of the total reflections selected randomly and never used in refinement.

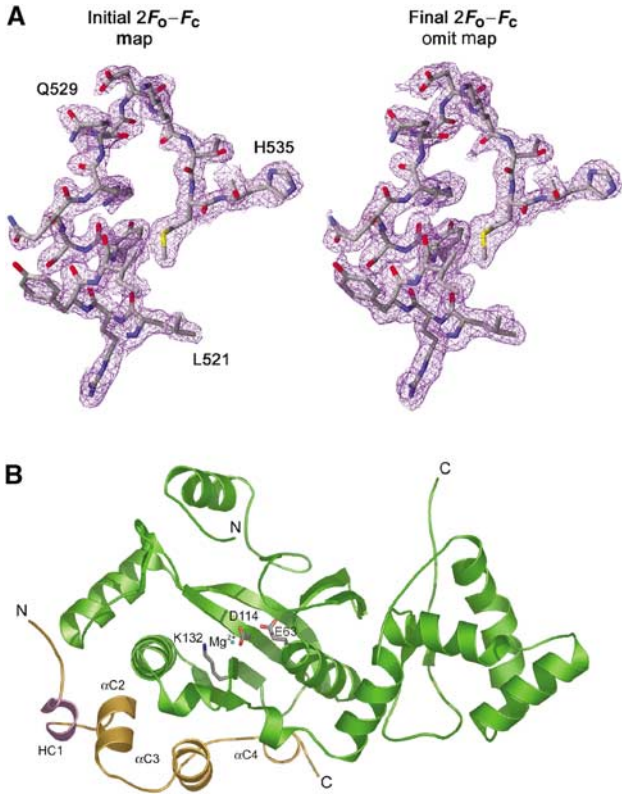

Figure 2 (**A**) TnsC(504–555) electron density. The atoms and bonds represent the final refined structure of residues 521–535 of the TnsC fragment. Gray, red, blue, and yellow atoms represent carbon, oxygen, nitrogen, and sulfur, respectively. The initial $2F_o-F_c$ map was calculated after simulated annealing, energy minimization, and *B* factor refinement using only the two TnsA molecules from the molecular replacement solutions. The final map is a simulated annealed omit map, where atoms from one of the two TnsC fragments within the asymmetric unit were omitted from the map calculation. Residues L521, Q529, and H535 are shown for frame of reference. (**B**) Ribbon diagram of the complex. The Cα trace of TnsA is shown in green, and that of TnsC(504–555) in gold. The N- and C-termini of each chain are labeled. Side chains of residues that define the TnsA active site and bound Mg^{2+} are shown, where white, red, dark blue, and light blue represent carbon, oxygen, nitrogen, and magnesium, respectively. The secondary structure of TnsC(504–555) was assigned using the dss algorithm as implemented in PyMOL (www.pymol.org). The N-terminal helix of TnsC(504–555), designated HC1 and colored violet, is a 3_{10} helix, and the other three are α-helices.

residues 506–552. The final model was refined to an *R* factor of 21.1% with excellent geometry.

As shown in Figure 2B, TnsC(504–555) interacts exclusively with the N-terminal catalytic domain of TnsA (residues 1–169), resulting in a calculated buried surface area between TnsA and TnsC(504–555) of 1180 Å^2. The conformation of the TnsC fragment is highly extended, reminiscent of the Greek letter **Ω**, and the only secondary structure elements are four short helices (designated HC1 and αC2–αC4). As a result, the fragment lacks anything resembling a globular form or a hydrophobic core. A search for related structures using the Dali server (Holm and Sander, 1997) indicated that the TnsA-bound conformation of TnsC(504–555) has no three-dimensional structural homologues.

One notable structural consequence of the binding of TnsC(504–555) to TnsA is the burial of most of a large, exposed hydrophobic surface on TnsA (Figure 3). This ~1400 Å^2 contiguous hydrophobic surface (calculated with Grasp 1.3.6; Nicholls *et al*, 1991) was one of the most striking features of uncomplexed TnsA, as extensive hydrophobic surfaces are rarely encountered in water-soluble protein molecules. As a result of complex formation, polar residues of TnsC(504–555) face toward the solvent and, viewed as a single unit, the complex displays surface characteristics usually seen in soluble proteins.

At the interface between TnsA and TnsC(504–555), approximately 80% of the close contacts are hydrophobic interactions, whereas the remainder are predominantly polar with only two salt bridges present at the interface. Four residues of TnsC (V545, M547, L550, and F551) protrude deeply into a hydrophobic pit on the surface of TnsA (Figure 3) where they account for half of the van der Waals contacts between the binding partners and probably provide most of the binding free energy for complex formation.

Comparison of TnsA bound to TnsC(504–555) and free TnsA

When the structure of TnsA bound to TnsC(504–555) is compared with that of uncomplexed TnsA (Hickman *et al*, 2000), the two structures can be three-dimensionally superimposed with an r.m.s. deviation in 261 Cα positions of only 0.94 Å, indicating that binding does not induce significant conformational changes in TnsA. In particular, the active site of TnsA is unaltered by binding of TnsC(504–555), as superposition using atoms from the three essential active site residues of TnsA (E63, D114, and K132) gives an r.m.s. deviation of only 0.42 Å.

One interesting difference between the two structures is that the uncomplexed form of TnsA has two Mg^{2+} ions coordinated at the active site in a configuration similar to that seen in restriction endonucleases (Aggarwal, 1995;

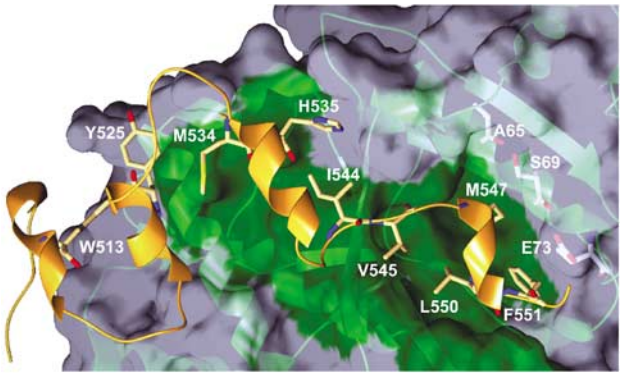

Figure 3 Van der Waals interactions. The molecular surface of TnsA is shown where green represents surface-exposed hydrophobic residues. Gray represents polar or charged residues. The Cα trace of TnsC(504–555) is shown in gold, while that of TnsA is shown in green. TnsC residues involved in important hydrophobic interactions are shown. Peach, red, blue, and yellow represent carbon, oxygen, nitrogen, and sulfur, respectively. Residues representing the positions of TnsA gain-of-function mutations (A65, S69, and E73) are shown with white carbon atoms.

Kovall and Matthews, 1999), whereas the TnsA/TnsC (504–555) complex has only one of these metal ions. The presence of even one Mg^{2+} ion in the active site is surprising because there is no Mg^{2+} in the crystallization buffer of the complex. However, the complex was exposed to 50 mM $MgSO_4$ during gel filtration; Mg^{2+} was presumably acquired at this step and remained bound during subsequent dialysis prior to crystallization (see Materials and methods). Its presence indicates that this metal ion binds particularly tightly, and implies a substantially larger dissociation constant for the second Mg^{2+} ion observed in the original TnsA structure.

Location of TnsA gain-of-function mutants

The structure of the TnsA/TnsC(504–555) complex provides a framework for rationalizing the effects of a set of TnsA mutants known as the Class I gain-of-function mutants (Stellwagen and Craig, 1997a). The identification of gain-of-function mutants in the Tn7-encoded proteins has been a valuable tool in the study of their roles during transposition, both *in vitro* and *in vivo*. Gain-of-function mutants are those that allow parts of the Tn7 transposition reaction to proceed in the absence of the full complement of four Tn7-encoded proteins. For example, A225V in TnsC is a gain-of-function mutant as transposition now occurs in the absence of either of the targeting proteins, TnsD or TnsE, albeit with loss of targeting specificity (Stellwagen and Craig, 1997a).

Both gain-of-function and loss-of-function mutants have been identified in TnsA. Class I gain-of-function mutants (A65V, S69N, and E73K) are located on one face of an α-helix in the N-terminal domain of TnsA as shown in Figure 3 and allow the activation of the TnsAB transposase by TnsC in the absence of either TnsD or TnsE. The structure of the TnsA/TnsC(504–555) complex demonstrates that residues 65, 69, and 73 are all located at the interface between TnsA and TnsC, and therefore are appropriately positioned to modulate the interaction between TnsA and TnsC.

Examination of the structural environments of A65, S69, and E73 within the context of the TnsA/TnsC(504–555) complex suggests that the amino-acid substitutions in TnsA that lead to the Class I gain-of-function phenotype are more likely to disrupt the TnsA/TnsC interaction than to enhance it. Our attempts to test this hypothesis have been confounded by our inability to produce sufficient quantities of the TnsA Class I mutants for crystallization studies or for the direct measurement of binding constants to TnsC by sedimentation equilibrium or isothermal titration calorimetry. All three Class I gain-of-function mutants are expressed at lower levels in *E. coli* than wild-type TnsA, are less soluble, and tend to aggregate in solution. Nevertheless, preliminary gel filtration studies with limited amounts of E73K and S69N TnsA in the presence of TnsC(495–555) indicate that the gain-of-function mutants retain the ability to bind and comigrate with TnsC (data not shown). Further insight awaits more direct structural information.

Model of TnsA/TnsC(495–555) bound to DNA

The TnsC(504–555) fragment contains a number of basic residues ($pI_{calc} = 9.65$), many of which are surface exposed in the TnsA/TnsC(504–555) complex. This observation led us to consider whether they may contribute to DNA binding within the intact transpososome and, in particular, to transposon end binding by TnsA. We had previously proposed a model for DNA binding by TnsA, based on its structural homology with type II restriction enzymes for which there exists a large amount of three-dimensional structural information for their complexes with nucleic acids. Examination of the TnsA/TnsC(504–555) complex in the light of this TnsA/DNA model indicates that the observed conformation of TnsC(504–555) in the TnsA/TnsC(504–555) complex does not sterically interfere with the previously proposed DNA binding mode in the TnsA active site. In fact, numerous TnsC side chains—particularly in the N-terminal half of the TnsC(504–555) fragment—appear well-positioned to interact potentially with DNA phosphate groups.

The second intriguing result revealed by the structure of the complex is that TnsC residues 505–511 are close to the TnsB cleavage site (Figure 4B). The location of the TnsB cleavage site is necessarily established by a structural model for donor DNA binding in the TnsA active site because the TnsA and TnsB cleavage sites are staggered by only 3 bp, on opposite strands at each transposon end. We also noted that residues 505–511 are flanked on their C-terminal side by helix HC1, consisting of residues 512–516. On their N-terminal side, a multiple sequence alignment of TnsC with homologues from related transposons using Clustal W (Thompson *et al*, 1994) (Figure 4A) reveals a conserved cluster of positively charged residues (i.e., residues 495–501 of TnsC). Interestingly, if helix HC1 is extended upstream to include residues 505–511 and the cluster of basic amino acids beginning at residue 495, this modeled helix would block access of TnsB to its cleavage site (see figure in Supplementary data). However, if this modeled helix is slightly reoriented, it would be appropriately placed to interact with DNA and to allow TnsB to bind and cleave at the appropriate site on the transposon as shown in Figure 4B. In this model, the extended HC1 helix consisting of residues 495–516 is close enough to interact with DNA using multiple basic side chains, yet no longer physically blocks the TnsB cleavage site.

Hydroxyl radical footprinting studies of TnsB on Tn7 donor DNA indicate that several bases located adjacent to the TnsB cleavage site are readily accessible to solvent

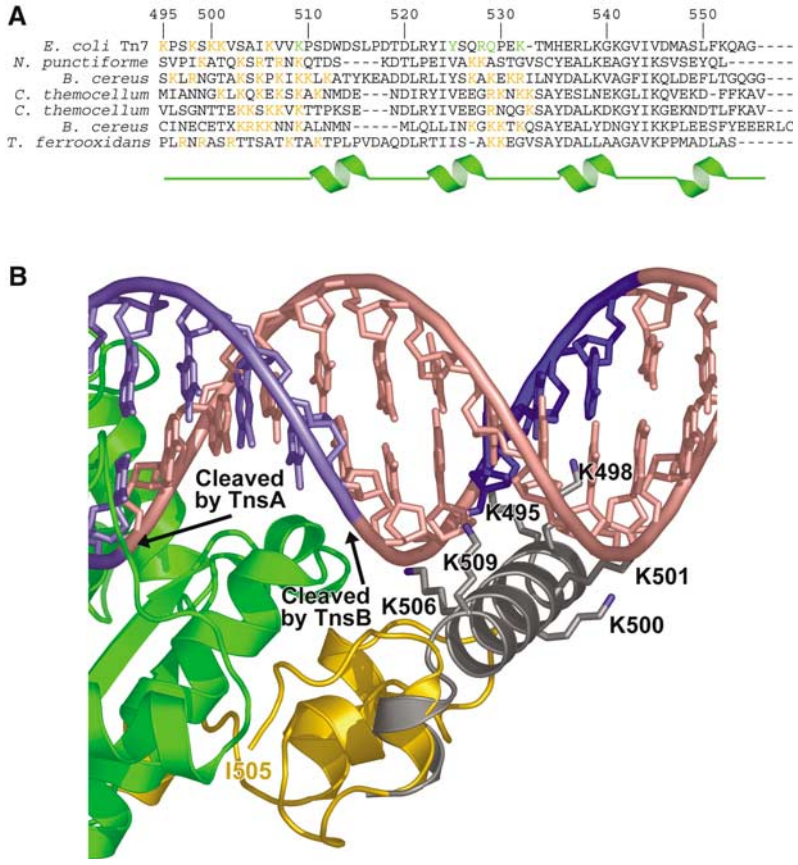

Figure 4 (**A**) Primary sequence alignment of TnsC and its homologues. Shown is an alignment of sequences representing the ~60 C-terminal residues of TnsC from Tn7 and its known homologues. The numbering corresponds to that of Tn7 TnsC. Residues highlighted in gold are basic residues predicted from sequence only to interact with phosphate backbone moieties of the DNA. Residues highlighted in green represent residues predicted to interact with DNA based on the TnsA/TnsC(504–555) structure. (**B**) Model of TnsA/TnsC(495–555) complex bound to DNA. The green and gold ribbons represent the Cα traces of TnsA and TnsC(504–555), respectively, from the solved crystal structure. The N-terminus of the observed TnsC(504–555) is labeled with I505. The dark gray ribbon represents the modeled residues 495–516 of TnsC, proposed to form a kinked α-helix. The salmon-colored region of the modeled DNA represents Tn7 donor DNA. On the left, the light blue DNA strands represent those bonds corresponding to flanking DNA. On the right, the navy blue bonds of the DNA strand cleaved by TnsB indicate a region of protection afforded by TnsB during hydroxyl radical footprinting. Modeled side chains predicted to interact directly with DNA are labeled with black lettering. The locations of the bonds cleaved by TnsA and TnsB are indicated.

(Arciszewska *et al*, 1991). Specifically, on the DNA strand cleaved by TnsB, the three bases just inside the TnsB cleavage site are solvent accessible, whereas on the opposite strand, five bases inside the TnsB cleavage site are exposed. Thus, even in the presence of TnsB, there is adequate space adjacent to its cleavage site to accommodate the modeled α-helix from TnsC.

The model presented in Figure 4B suggests a number of experimentally testable hypotheses with regard to the biochemical effect of TnsC(495–555). To investigate these, we have measured the effect of TnsC(495–555) on the DNA binding activity of TnsA and on the endonuclease activities of the TnsAB transposase.

DNA binding by the TnsA/TnsC(495–555) complex

The crystal structure of the TnsA/TnsC(504–555) complex reveals that one effect of complex formation is to bring a number of basic residues, provided by TnsC, close to the active site of TnsA. This observation suggested that TnsC might play a role in DNA donor binding. This possibility is appealing because it is well established that purified TnsB binds site specifically to transposon ends, yet DNA binding by TnsA alone has not been detected (Arciszewska *et al*, 1991; Bainton *et al*, 1993).

The ability of the TnsA/TnsC(495–555) complex to interact with DNA was examined using electrophoretic mobility shift assays. As shown in Figure 5A, the individual proteins do not bind DNA (lanes 1, 3, and 6), whereas the TnsA/TnsC(495–555) complex binds DNA strongly (lane 4). This effect is not specific for the Tn7 left and right ends as the gel shift can be competed by dI–dC (Figure 5B, lanes 8–10). In contrast, TnsA/TnsC(504–555) does not bind DNA (Figure 5A, lane 2), indicating a critical role for the additional positive charge cluster between residues 495 and 503.

To assess the importance of these positively charged residues, a mutant version of TnsC(495–555) was generated (designated TnsC(495–555)*) in which K495, K498, K500, K501, K506, and K509 were replaced with alanine residues. TnsC(495–555)* retains the ability to bind to TnsA as indicated by comigration on size exclusion chromatography (data not shown). Electrophoretic mobility shift assays with TnsA/TnsC(495–555)* conducted under identical conditions to those with unmutated TnsA/TnsC(495–555) demonstrated that the mutant version does not bind DNA (Figure 5A, lanes

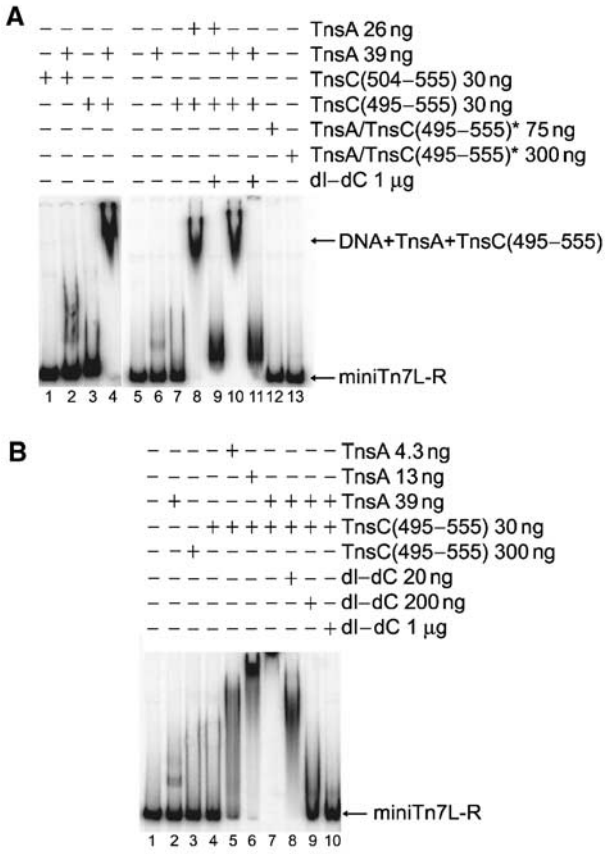

Figure 5 Gel mobility shift assays of TnsA and TnsC(495–555) on DNA. (**A**) The protein components added to the labeled miniTn7L-R DNA substrate are as indicated. In lanes 1–11, TnsA, TnsC(504–555), and TnsC(495–555) were added separately and in the amounts indicated. In lanes 12 and 13, TnsA and TnsC(495–555)* were added as a complex coeluted from a gel filtration column. (**B**) The protein components and poly(dI–dC) were added to the labeled miniTn7L-R DNA as indicated for lanes 1–10.

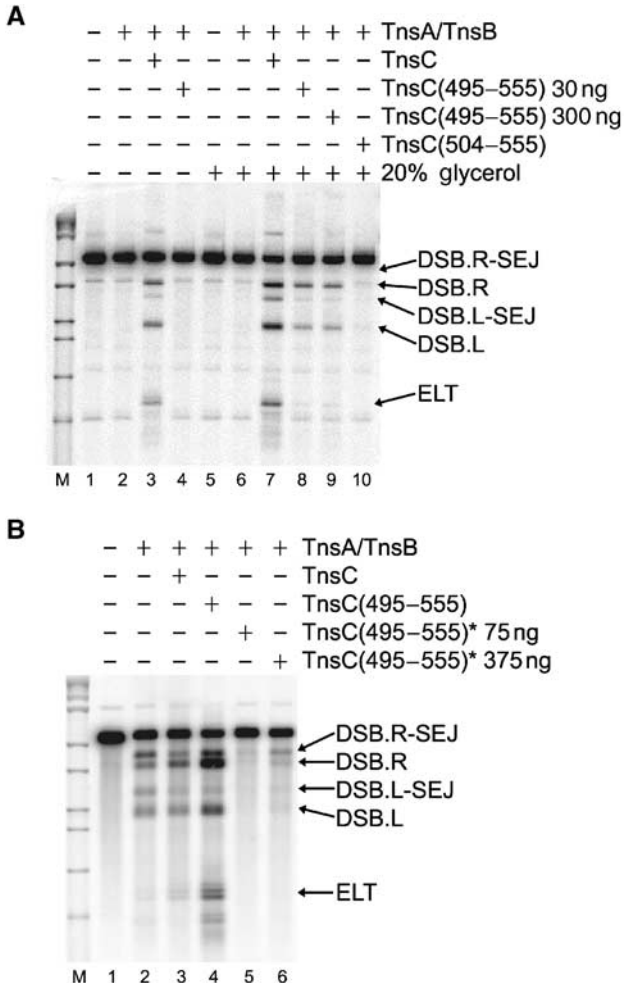

Figure 6 (**A**) Effect of TnsC(1–555), TnsC(495–555), and TnsC(504–555) on TnsAB donor cleavage activities in the presence of 15 mM Mg^{2+}, with and without 20% glycerol. *In vitro* transposition reactions of TnsA/TnsB or TnsA/TnsB/TnsC were performed and the recombination products were separated using a 1.2% agarose gel. DSBs of donor DNA at the right end of Tn7 (Tn7R) or the left end (Tn7L) result in DSB.R and DSB.L, respectively. An ELT is the result of DSB at both ends. The single end joined products (SEJ) are a result of an intramolecular-joining reaction, where an exposed end of the transposon attacks its opposite end. (**B**) Effect of TnsC, TnsC(495–555), and TnsC(495–555)* on TnsAB donor cleavage activities in the presence of 1.5 mM Mn^{2+} and 20% glycerol. Assays were performed in a similar manner as those in panel A. Lanes 5 and 6 contain the preformed TnsA/TnsC(495–555)* complex purified by coelution from a gel filtration column, whereas the protein components for the other reactions were added separately.

12 and 13). Subsequent double-stranded DNA cleavage (DSB) assays also showed that the TnsA/TnsC(495–555)* complex was unable to stimulate cleavage of donor DNA (Figure 6B, lanes 5 and 6). It would be interesting to determine if mutating only a subset of the six lysine residues would have a similar effect.

DNA cleavage activity of the TnsA/TnsC(504–555) and TnsA/TnsC(495–555) complexes

To examine the effects of the C-terminal fragments of TnsC on TnsA and TnsB cleavage activities, a TnsABC DSB assay was employed using purified Tn7 proteins and a plasmid containing a mini-Tn7 element (Biery *et al*, 2000). For the transposition reaction to take place, DSBs must occur at both ends of the transposon; these are generated by TnsA cleavage at the 5′ ends and TnsB cleavage at the 3′ ends. The product of appropriate cleavage reactions at both ends of the transposon is an excised linear transposon (ELT).

As shown in Figure 6A and consistent with previous results (Bainton *et al*, 1993), in the presence of Mg^{2+}, TnsA and TnsB are not able to produce the ELT product (lane 2). However, transposon excision is stimulated by the addition of full-length TnsC (lane 3), an effect that is further enhanced by glycerol (lane 7). The addition of TnsC(495–555) slightly stimulates ELT production (lanes 8 and 9), although to a lesser extent than that seen with full-length TnsC. In contrast, no ELT products are formed with the shorter TnsC(504–555) fragment (lane 10).

When Mg^{2+} is replaced with Mn^{2+} in the assay buffer, it has been shown that a low level of transposon excision can now be detected in the presence of only TnsA and TnsB (Biery *et al*, 2000). We therefore repeated the TnsABC DSB assays to determine if the TnsC fragments could stimulate ELT production under these modified conditions (Figure 6B). As in the Mg^{2+} buffer, full-length TnsC stimulates transposon excision (lane 3) when compared to the level observed with TnsA and TnsB (lane 2). However, TnsC(495–555) stimulates cleavage of the donor ends (lane 4) to an even greater extent

than that seen with full-length TnsC. Thus, the ability of TnsC to stimulate the cleavage activities of the TnsAB transposase resides within the last 60 C-terminal residues of TnsC.

Although we cannot account for the dramatic stimulation by TnsC(495–555) compared to full-length TnsC in Mn^{2+} but not Mg^{2+}, a differential effect of Mn^{2+} on catalytic activities is well documented for other metal-dependent nuclease enzymes studied *in vitro* (Cowan, 1998).

Stabilization of TnsA by the TnsC(495–555) polypeptide

During the course of our previous structural work with TnsA (Hickman *et al*, 2000), we observed that concentrated solutions of purified TnsA rapidly precipitated at room temperature. As a result, all TnsA experiments were conducted at 4°C. In contrast, the TnsA/TnsC(504–555) complex was crystallized at 20°C and, even after several days at this temperature, there was no evidence of aggregation. Intrigued by this difference in solution behavior, we investigated this qualitative observation using differential scanning calorimetry (DSC) to obtain quantitative data.

The changes in heat capacity as a function of increasing temperature of TnsA alone and the TnsA/TnsC(495–555) complex are shown in Figure 7. The transition temperature (T_m) for TnsA was measured to be 39.9°C, whereas the T_m for the complex is 58.7°C. This dramatic 19°C increase in the thermal stability is almost twice the average ΔT_m of ~10°C for known protein/polypeptide systems. It is also greater than the 16°C reported for the bovine β trypsin/soybean trypsin inhibitor complex, which exhibits one of the largest measured ΔT_m for a protein/polypeptide complex (Donovan and Beardslee, 1975). The magnitude of the ΔT_m between TnsA and TnsA/TnsC(495–555) is even more notable as only ~1180 Å^2 is buried in the TnsA/TnsC(495–555) complex compared to ~1450 Å^2 of accessible surface area buried in the interface of the bovine β trypsin/soybean trypsin inhibitor complex (Janin and Chothia, 1990).

The observation that the T_m for uncomplexed TnsA is 39.9°C indicates that at 37°C, if TnsA is not associated with TnsC, it is likely to be at least partially denatured. This previously unsuspected effect of complex formation provides yet another mechanism by which TnsC can control the assembly and function of the Tn7 transpososome.

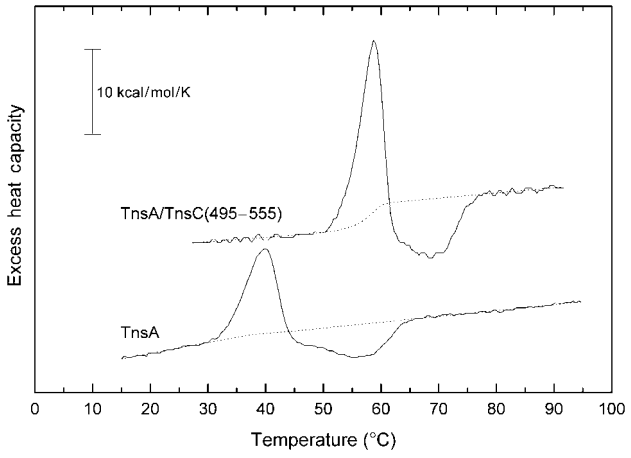

Figure 7 TnsC(495–555) significantly increases the thermal stability of TnsA. Excess heat capacity versus temperature profile for TnsA alone and the TnsA/TnsC(495–555) complex from DSC experiments is shown.

The position of the pre- and post-transition baselines in Figure 7 indicate that there is a large heat capacity increase of ~2.8 kcal/mol/K associated with the denaturation of the TnsA/TnsC(495–555) complex. In contrast, there is little or negligible heat capacity change upon denaturation of TnsA alone. This result is consistent with the observation that there are a large number of hydrophobic groups buried at the contact interface, which become exposed to solvent upon dissociation and denaturation of the complex. Another contributor to the observed increase in heat capacity may be conformational changes of TnsC(495–555) upon dissociation.

The finding that there is marked thermal stabilization of TnsA upon complex formation with TnsC(495–555) led us to revisit protease digestion results that identified residues of TnsA that were protected when it was bound to TnsC (Lu and Craig, 2000). We were initially disconcerted that there was no obvious explanation from the TnsA/TnsC(504–555) crystal structure for the protease protection data that identified sites of protection throughout the TnsA N-terminal domain (Figure 8A), none of which are contacted by TnsC(504–555). However, noting that the experiments were performed at 37°C, we wondered if the protease protection conferred by TnsC was a result of occlusion of a portion of TnsA or if it could be attributed to overall stabilization of the protein. We therefore repeated the digestion experiments with the TnsA/TnsC(495–555) complex under conditions identical to those used by Lu and Craig for the full-length proteins. As shown in Figure 8B, TnsA alone is rapidly digested by chymotrypsin and trypsin to form a ladder of proteolysis products. In contrast, TnsC(495–555) prevented the formation of these products and protected those same regions of TnsA as does full-length TnsC. Thus, a likely explanation for the protease protection data is that TnsC(495–555) has a global effect and not a local effect on TnsA by increasing its structural stability.

The stability of the Tn7 transpososome has recently been examined by Skelding *et al* (2002), who showed that the addition of TnsA to a preformed complex of TnsBC + D, target DNA, and donor DNA significantly stabilizes the entire nucleoprotein complex. When a preassembled complex is exposed to a 40°C temperature challenge for 10 min, 90% of the complex remains intact if TnsA is present. In contrast, none of the complex remains intact if TnsA is not added. Thus, at physiological temperatures, it appears that TnsA reciprocates the stabilization afforded to it through its interaction with TnsC by increasing the stability of the entire Tn7 nucleoprotein complex.

Conclusion

Lu and Craig (2000) have previously suggested several possible roles for TnsC in activating the TnsAB transposase: that it may introduce a conformational change in the catalytic sites of the transposase components, that it could facilitate TnsA and TnsB assembly on the transposon ends, or that it is a part of the transposase itself. Our results presented here address all three of these possibilities.

Protease digestion results combined with gel filtration indicate that the only portion of TnsC that binds stably to TnsA is the region corresponding to residues 504–555. The high-resolution crystal structure of the complex between TnsA and TnsC(504–555) reveals that binding is not associated with a conformational change in TnsA. Although we

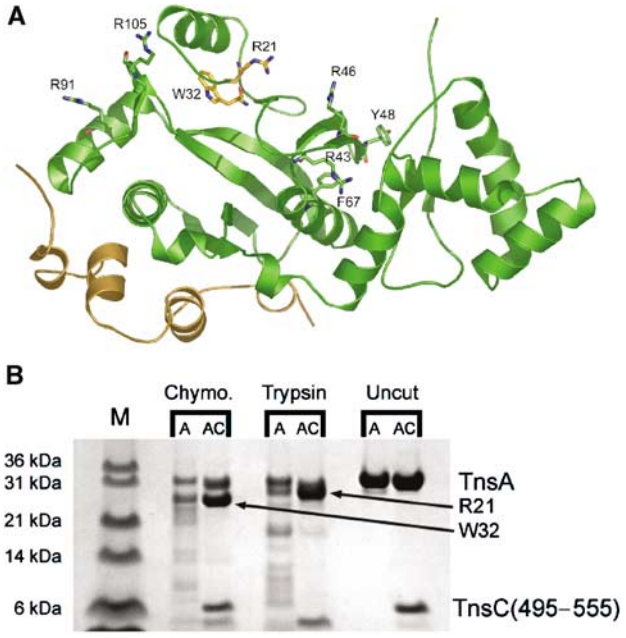

Figure 8 (**A**) Trypsin and chymotrypsin cleavage sites on TnsA. Shown is a ribbon diagram of the TnsA/TnsC(504–555) complex where green represents the TnsA backbone and gold represents that of TnsC(504–555). The side chains represent positions cleaved in TnsA by either trypsin or chymotrypsin. Upon addition of full-length TnsC or TnsC(495–555), protection is afforded to residues represented by side chains with green carbon atoms, and significant cleavage occurs only after R21 and W32, shown with gold carbon atoms. (**B**) Protease digest of TnsA compared to that of the TnsA/TnsC(495–555) complex. Chymotrypsin and trypsin digests are labeled. Digestions containing only TnsA are labelled A and those containing the TnsA/TnsC(495–555) complex are labelled AC. R21 and W32 indicate fragments resulting from cleavage after R21 (trypsin digest) and W32 (chymotrypsin digest), respectively. Uncut controls are shown on the right.

have not confirmed this observation with the two full-length proteins, we have been unable to detect an interaction between TnsA and TnsC(1–503), and it appears unlikely that any effect of TnsC on the catalytic activity of TnsA is transduced through a structural change in TnsA. Rather, modeling based on the crystal structure of the complex, combined with the observed location of basic residues of TnsC, provided a structural basis for hypothesizing a role of TnsC in aiding donor DNA binding by TnsA.

Here we have shown that the C-terminal region of TnsC, residues 495–555, confers upon TnsA the ability to bind donor DNA. In other transposition systems, the catalytic center is separated from nonspecific DNA binding functions on the basis of domain structure. For example, in HIV integrase, the central catalytic domain (residues 50–212) contains the enzyme active site, whereas the C-terminal domain (residues 213–288) binds DNA nonspecifically (Craigie, 2002). It now appears that the separation of these functions in TnsA is even more elaborate: only when TnsA is bound to TnsC is the resulting complex capable of DNA binding. This presumably ensures that TnsA's substrate remains unavailable for cleavage until the entire transpososome has been assembled (or, at least, until TnsA and TnsC are associated).

We have also shown that TnsC(495–555) stimulates the cleavage activities of the TnsAB transposase as measured by transposon excision assays. This may well be a combined effect of donor DNA binding by the TnsA/TnsC(495–555) complex and stabilization of the catalytic domain of TnsA by the C-terminal fragment of TnsC.

The dramatic thermal stabilization conferred upon TnsA by TnsC(495–555) raises a number of intriguing questions: are TnsA and TnsC ever found separately in cells? If so, how then is TnsA stabilized? Genetic studies indicate that while *tnsA* and *tnsB* form an operon, expression of the other *tns* genes is not entirely dependent on the *tnsAB* promoter (Waddell and Craig, 1988). It would be interesting to investigate the temporal appearance of the Tns proteins and their localization relative to each other *in vivo*.

We continue to refine our picture of how TnsC acts as the crucial bridge between target and donor DNA during Tn7 transposition. The central regulatory function of TnsC is necessarily mediated by structural interactions with other Tn7 proteins; here we have provided the first three-dimensional view of the protein–protein interactions that link TnsC to the TnsA component of the transposase.

Materials and methods

Purification and peptide characterization

The *tnsA* gene was placed between the *Nde*I and *Bam*HI sites of pET-28b (Novagen). The *tnsC* gene was placed between the *Nco*I and *Eco*RI sites of pET-28b (Novagen). The TnsC(1–503) construct was produced by replacing codon 504 with a TGA codon using site-directed mutagenesis of the full-length TnsC. The portion of the *tnsC* gene encoding residues 504–555 was ligated between the *Eco*RV and *Eco*RI sites of pET-32b (Novagen). The fusion construct was altered using site-directed mutagenesis to eliminate the enterokinase cleavage site and later to add the sequence coding for residues 495–503 of TnsC.

Separate cultures of BL21(DE3) cells were grown at 37°C in LB broth until slightly turbid. Subsequent chilling of the cultures to 12°C, growth to an OD600nm of approximately 0.8, and addition of IPTG to a final concentration of 0.25 mM resulted in the expression of soluble TnsA, untagged TnsC, TrxA-TnsC(504–555), TrxA-TnsC(495–555), and TrxA-TnsC(495–555)*.

Cells were harvested after 24 h and resuspended in metal chelation binding buffer (MCB: 20 mM Tris pH 8.0, 10% (v/v) glycerol, 1 M NaCl, and 25 mM imidazole). All purification steps were performed at 4°C. For the copurification of TnsA and full-length TnsC, the cells from both cultures were combined and β-mercaptoethanol (β-ME) was added to a final concentration of 3 mM just prior to lysis by sonication. Cell debris was removed by centrifugation. The soluble material was loaded onto a HiTrap metal chelation column (Amersham Biosciences) that had been equilibrated first with $NiSO_4$, then MCB. After extensive washing, bound protein was eluted with metal chelation elution buffer (20 mM Tris pH 8.0, 10% (v/v) glycerol, 1 M NaCl, and 200 mM imidazole).

The TnsA/C complex was cleaved with thrombin for 16 h during dialysis against MCB. Thrombin was removed with benzamidine sepharose 6B resin (Amersham Biosciences). The polyhistidine tag was removed using a HiTrap metal chelation column equilibrated with $NiSO_4$, then MCB.

Protein in the flow-through was dialyzed into heparin binding buffer (HB: 10 mM sodium phosphate pH 7.0, 100 mM NaCl, 10% (v/v) glycerol, and 5 mM β-ME), then loaded onto a HiPrep Heparin FF column (Amersham Biosciences). Protein was eluted with a NaCl gradient from 0 to 1.0 M over four column volumes.

Eluted protein was dialyzed against TSK β buffer (TSK-β: 20 mM Tris pH 7.5, 50 mM $MgSO_4$, 500 mM NaCl, 10% (v/v) glycerol, and 5 mM β-ME), concentrated, and then loaded onto a TSK-Gel G3000SW column (TosoHaas), which had been previously equilibrated with TSK α buffer (TSK-α: 20 mM Tris pH 7.5, 50 mM $MgSO_4$, 500 mM NaCl, 10% (v/v) glycerol, and 2 mM dithiothreitol (DTT)). Fractions containing the TnsA/TnsC complex were pooled and concentrated to 10 mg/ml.

The purification of the TnsA/TnsC(504–555) complex was performed in a similar manner as the full-length TnsA/TnsC

complex. However, slight changes were made to the purification protocol. Briefly, each protein was purified separately on a metal chelation column. Eluted proteins were dialyzed into cation exchange buffer (10 mM sodium citrate pH 5.5, 5 mM EDTA, and 5 mM β-ME), then subjected to cation exchange chromatography using a POROS HS/M column (Applied Biosystems). Proteins were eluted with a NaCl gradient from 0 to 1.0 M over 2.5 column volumes and then combined. Affinity tags were cleaved using thrombin as described above. After elution through benzamidine sepharose and a HiTrap metal chelation column, the complex was dialyzed into TSK-β. After gel filtration on TSK-Gel G3000SW, purified TnsA/TnsC(504–555) was dialyzed for ~16 h against buffer containing only 200 mM sodium malonate and 5 mM DTT prior to crystallization.

For the limited proteolysis of the full-length TnsA/TnsC complex, 500 μl of purified TnsA/TnsC complex at 5 mg/ml in TSK-α was cleaved with 4 μg of papain on ice for 4 h. The cleavage products were subjected to gel filtration on a Superdex 200 column (Amersham Biosciences) using TSK-α. Fractions from the eluted peaks were run on a denaturing 4–12% NuPAGE gel (Invitrogen).

For N-terminal sequencing of the TnsC fragments, cleaved sample was run on a denaturing PAGE gel, then transferred onto a polyvinylidene difluoride membrane. Protein bands were visualized by staining with Coomassie brilliant blue, then subjected to N-terminal sequencing on a Hewlett Packard 241 Protein Sequencer.

For MALDI-TOF, the cleaved TnsA/TnsC complex was dialyzed for 8 h against 5% acetic acid. The soluble fraction was then mixed with matrix solution (10 mg/ml sinapinic acid, 30% acetonitrile, and 0.07% TFA) at a 9:1 ratio of matrix to sample. A volume of 4 μl of the mixture was dried on the sample plate and MALDI-TOF data were collected on a Voyager-DE Biospectrometry Workstation (Applied Biosystems).

DSB assays

The TnsABC reactions contained 0.25 nM donor DNA, Tns proteins, and buffer. The donor DNA, a [α-^{32}P]dCTP-labeled 5.9 kb plasmid named pEMΔ, contains a 1.6 kb miniTn7Km^{R} element (kanamycin gene segment between 166 bp Tn7L and 199 bp Tn7R ends). The Tns proteins include 39 ng of TnsA, 25 ng of TnsB, and 30 ng of either full-length or truncated TnsC. The buffers contain 20 mM Tris (pH 7.6), 0.9 mM HEPES (pH 8.0), 14 mM NaCl, 5 mM KCl, 16 μM EDTA, 2 mM DTT, 60 μg/ml bovine serum albumin (BSA), 100 μg/ml tRNA, 12 μM ATP, 120 μM CHAPS, 20 or 0.5% (as indicated in the figure) glycerol, 0.12 mM $MgCl_2$, and 15 mM MgAc or 1.5 mM $MnCl_2$. The reactions were performed at 30°C for 30 min in a final volume of 100 μl. DNA was extracted with phenol:chloroform (1:1), precipitated with ethanol, digested with *Alw*NI, *Apa*I, and RNAse, and analyzed on a 1.2% (w/v) agarose TBE gel, then Southern blotted. The blots were analyzed using a Molecular Dynamics PhosphorImager.

Gel mobility shift assay

The DNA substrate (mTn7L-R) is a 5′-γ-^{32}P-labeled 459 bp DNA fragment containing a 174 bp Tn7 left end, a 199 bp Tn7 right end, and a 43 bp flanking sequence on both ends. It was prepared by digesting pBM2 (which contains mTn7 and the Kan gene) with *Hin*cII to remove the Kan gene and religating to generate a plasmid containing the Tn7 left and right ends. This was then used as the template, and 43 bp flanking sequences were generated by PCR. The final 20 μl reaction mixture contains 25 mM HEPES, 2.5 mM Tris, 130 mM NaCl, 1 mM $MgCl_2$, 0.0625 mM EDTA, 4.4 mM DTT, 0.005% BSA, 0.1 mM ATP, 1 mM CHAPS, and 5% glycerol. A 1 μg portion of poly(dI–dC)·poly(dI–dC) and different amounts of TnsA, TnsC(495–555), and TnsC(495–555) lysine to alanine mutants were added as indicated in Figure 6. The DNA substrate is approximately 9 fmol per reaction. After 20 min incubation at 30°C, the protein–DNA complexes were analyzed by electrophoresis through a 5% polyacrylamide gel (37.5:1) in 0.5 × TBE buffer at 15 V/cm for 5 h. The gel was vacuum-dried and viewed with a Molecular Dynamics PhosphorImager.

Differential scanning calorimetry

Purified TnsA and purified TnsA/TnsC(495–555), between 1.3 and 2 mg/ml, were separately dialyzed against 10 mM sodium phosphate pH 7.2, 500 mM NaCl, 10% (v/v) glycerol, and 2 mM DTT. The temperature dependence of the difference in heat capacity between protein solutions and buffer alone was obtained by DSC using a Microcal (Springfield, MA) MC-2 calorimeter at a scan rate of 1.98 K/min. As the endotherms illustrate, denaturation is closely followed by an exothermic process, which we attribute to precipitation/aggregation. This later relaxes to the linear postdenaturation baseline. Upon reheating, no cooperative endotherm was observed, indicating that the denaturation was not reversible.

Analysis of these denaturation endotherms uses data only up to the peak of the experimental curve and assumes an A→B two-state model for the denaturation of TnsA and an A→2B model for the dissociation of the TnsA/TnsC(495–555) complex. Values of ΔH_{CAL} obtained by this method were 63 kcal/mol for the former and 96 kcal/mol for the latter.

Crystallization

Crystals of the TnsA/TnsC(504–555) complex were grown at 20°C using the hanging-drop method. Protein solution at 10 mg/ml was mixed at a 2:1 ratio with 1.4 M sodium malonate, 48 mM Li_2SO_4, 2% 2-methyl-2,4-pentanediol, and 5 mM DTT. Significant crystal growth ceased after 5 days.

Data collection, structure determination, and refinement

Crystals were cryoprotected with Paratone-N (Hampton Research) and flash-cooled to 95 K using liquid nitrogen. Diffraction data were collected at beamline 22-ID in the facilities of the South East Regional Collaborative Access Team (SER-CAT) at the Advanced Photon Source, Argonne National Laboratories on a MAR165 CCD detector using X-rays at a wavelength of 1.0 Å. Crystals were of the space group C2 with unit-cell parameters $a = 156.04$ Å, $b = 70.13$ Å, $c = 89.68$ Å, and $\beta = 123.61°$. Data were reduced using HKL2000 (Otwinowski and Minor, 1997). Two TnsA/TnsC(504–555) complexes are in each asymmetric unit. A TnsA monomer (accession code 1F1Z) was used as a search model in the program AMoRe (Navaza, 1994) to obtain a molecular replacement solution for protein phases. The electron density for TnsC(504–555) was readily interpretable after an initial rigid body refinement and simulated annealing of the TnsA molecule using CNS (Brünger *et al*, 1998). After building the TnsC(504–555) polypeptide, refinement proceeded with simulated annealing, energy minimization, and individual *B* factor refinement. Water molecules were picked utilizing the water pick protocol in CNS and manually confirmed or rejected upon inspection using the program O (Jones *et al*, 1991).

Protease footprinting

Assays were performed as reported previously (Lu and Craig, 2000), with changes in protein concentration to facilitate better observation of bands in the gel. Chymotrypsin digests were performed at 37°C for 15 min by adding 160 ng chymotrypsin to a solution containing 12 μg of either TnsA or TnsA/TnsC(495–555). Trypsin digests were performed at 37°C for 5 min by adding 80 ng of trypsin to 12 μg of either TnsA or TnsA/TnsC(495–555) complex.

Supplementary data

Supplementary data are available at *The EMBO Journal* Online.

Acknowledgements

We thank C Bradley for helpful comments and R Ghirlando for sedimentation equilibration measurements. Use of the Advanced Photon Source was supported by the US Department of Energy, Office of Science, and Office of Basic Energy Sciences, under contract no. W-31-109-Eng-38.

Protein Data Bank ID Code

Coordinates and structure factors have been deposited with the Protein Data Bank (ID code 1T0F).

References

Aggarwal AK (1995) Structure and function of restriction endonucleases. *Curr Opin Struct Biol* **5:** 11–19

Arciszewska L, McKown RL, Craig NL (1991) Purification of TnsB, a transposition protein that binds to the ends of Tn7. *J Biol Chem* **266:** 21736–21744

Bainton RJ, Kubo KM, Feng JN, Craig NL (1993) Tn7 transposition—target DNA recognition is mediated by multiple Tn7-encoded proteins in a purified *in vitro* system. *Cell* **72:** 931–943

Biery MC, Lopata M, Craig NL (2000) A minimal system for Tn7 transposition: the transposon-encoded proteins TnsA and TnsB can execute DNA breakage and joining reactions that generate circularized Tn7 species. *J Mol Biol* **297:** 25–37

Brünger AT, Adams PD, Clore GM, Delano WL, Gros P, Grosse-Kunstleve RW, Jiang J-S, Kuszewski J, Nilges M, Pannu NS, Read RJ, Rice LM, Simonson T, Warren GL (1998) Crystallography & NMR System: a new software suite for macromolecular structure determination. *Acta Crystallogr D* **54:** 905–921

Cowan JA (1998) Metal activation of enzymes in nucleic acid biochemistry. *Chem Rev* **98:** 1067–1087

Craig NL (2002) Tn7. In *Mobile DNA II*, Craig NL, Craigie R, Gellert M, Lambowitz AM (eds), pp 423–456. Washington, DC: ASM Press

Craigie R (2002) Retroviral DNA Integration. In *Mobile DNA II*, Craig NL, Craigie R, Gellert M, Lambowitz AM (eds), pp 613–630. Washington, DC: ASM Press

DeBoy RT, Craig NL (1996) Tn7 transposition as a probe of *cis* interactions between widely separated (190 kilobases apart) DNA sites in the *Escherichia coli* chromosome. *J Bacteriol* **178:** 6184–6191

Donovan JW, Beardslee RA (1975) Heat stabilization produced by protein–protein association. A differential scanning calorimetric study of the heat denaturation of the trypsin–soybean trypsin inhibitor and trypsin–ovomucoid complexes. *J Biol Chem* **250:** 1966–1971

Dyda F, Hickman AB, Jenkins TM, Engelman A, Craigie R, Davies DR (1994) Crystal structure of the catalytic domain of HIV-1 integrase: similarity to other polynucleotidyl transferases. *Science* **266:** 1981–1986

Gamas P, Craig NL (1992) Purification and characterization of TnsC, a Tn7 transposition protein that binds ATP and DNA. *Nucleic Acids Res* **25:** 2525–2532

Hauer B, Shapiro JA (1984) Control of Tn7 transposition. *Mol Gen Genet* **194:** 149–158

Hickman AB, Li Y, Mathew SV, May EW, Craig NL, Dyda F (2000) Unexpected structural diversity in DNA recombination: the restriction endonuclease connection. *Mol Cell* **5:** 1025–1034

Holm L, Sander C (1997) Protein structure comparison by alignment of distance matrices. *J Mol Biol* **233:** 123–138

Janin J, Chothia C (1990) The structure of protein–protein recognition sites. *J Biol Chem* **265:** 16027–16030

Jones TA, Zou J-Y, Cowan SW, Kjeldgaard M (1991) Improved methods for building protein models in electron density maps and the location of errors in these models. *Acta Crystallogr A* **47:** 110–119

Kovall RA, Matthews BW (1999) Type II restriction endonucleases: structural, functional, and evolutionary relationships. *Curr Opin Chem Biol* **3:** 578–583

Kuduvalli PN, Rao JE, Craig NL (2001) Target DNA structure plays a critical role in Tn7 transposition. *EMBO J* **20:** 924–932

Lu F, Craig NL (2000) Isolation and characterization of Tn7 transposase gain-of-function mutants: a model for transposase activation. *EMBO J* **19:** 3446–3457

May EW, Craig NL (1996) Switching from cut-and-paste to replicative Tn7 transposition. *Science* **272:** 401–404

Navaza J (1994) AMoRe: an Automated Package for Molecular Replacement. *Acta Crystallogr A* **50:** 157–163

Nicholls A, Sharp KA, Honig B (1991) Protein folding and association: insights from the interfacial and thermodynamic properties of hydrocarbons. *Proteins* **11:** 281–296

Otwinowski Z, Minor W (1997) Processing of X-ray diffraction data collected in oscillation mode. *Methods Enzymol* **276:** 307–326

Peters JE, Craig NL (2001) Tn7: smarter than we thought. *Nat Rev Mol Cell Biol* **2:** 806–814

Rao JE, Miller PS, Craig NL (2000) Recognition of triple-helical DNA structures by transposon Tn7. *Proc Natl Acad Sci USA* **97:** 3936–3941

Sarnovsky RJ, May EW, Craig NL (1996) The Tn7 transposase is a heteromeric complex in which DNA breakage and joining activities are distributed between different gene products. *EMBO J* **15:** 6348–6361

Skelding Z, Sarnovsky R, Craig NL (2002) Formation of a nucleoprotein complex containing Tn7 and its target DNA regulates transposition initiation. *EMBO J* **21:** 3494–3504

Stellwagen AE, Craig NL (1997a) Gain-of-function mutations in TnsC, an ATP-dependent transposition protein that activates the bacterial transposon Tn7. *Genetics* **145:** 573–585

Stellwagen AE, Craig NL (1997b) Avoiding self: two Tn7-encoded proteins mediate target immunity in Tn7 transposition. *EMBO J* **16:** 6823–6834

Stellwagen AE, Craig NL (2001) Analysis of gain-of-function mutants of an ATP-dependent regulator of Tn7 transposition. *J Mol Biol* **305:** 633–642

Thompson JD, Higgins DG, Gibson TJ (1994) CLUSTAL W: improving the sensitivity of progressive multiple sequence alignment through sequence weighting, position-specific gap penalties, and weight matrix choice. *Nucleic Acids Res* **22:** 4673–4680

Waddell CS, Craig NL (1988) Tn7 transposition, two transposition pathways directed by five Tn7-encoded genes. *Genes Dev* **2:** 137–149